Water Research 123 (2017) 277–289

Contents lists available at ScienceDirect

Water Research

journal homepage: www.elsevier.com/locate/watres

Elucidating microbial community adaptation to anaerobic co-digestion of fats, oils, and grease and food waste

Yamrot M. Amha [a], Pooja Sinha [a], Jewls Lagman [a], Matt Gregori [b, c], Adam L. Smith [a, *]

[a] Astani Department of Civil and Environmental Engineering, University of Southern California, 3620 South Vermont Avenue, Los Angeles, CA 90089, USA
[b] Divert, Inc., 23 Bradford Street, Concord, MA 01742, USA
[c] Southern California Gas Company, 555 West Fifth Street, Los Angeles, CA 90013, USA

ARTICLE INFO

Article history:
Received 7 April 2017
Received in revised form
22 June 2017
Accepted 22 June 2017
Available online 23 June 2017

Keywords:
Anaerobic digestion
Microbial community
Illumina sequencing
Methane
Thermophilic

ABSTRACT

Despite growing interest in co-digestion and demonstrated process improvements (e.g., enhanced stability and biogas production), few studies have evaluated how co-digestion impacts the anaerobic digestion (AD) microbiome. Three sequential bench-scale respirometry experiments were conducted at thermophilic temperature (50 °C) with various combinations of primary sludge (PS); thickened waste activated sludge (TWAS); fats, oils, and grease (FOG); and food waste (FW). Two additional runs were then performed to evaluate microbial inhibition at higher organic fractions of FOG (30–60% volatile solids loading (VSL; v/v)). Co-digestion of PS, TWAS, FOG, and FW resulted in a 26% increase in methane production relative to digestion of PS and TWAS. A substantial lag time was observed in biogas production for vessels with FOG addition that decreased by more than half in later runs, likely due to adaptation of the microbial community. 30% FOG with 10% FW showed the highest increase in methane production, increasing 53% compared to digestion of PS and TWAS. FOG addition above 50% VSL was found to be inhibitory with and without FW addition and resulted in volatile fatty acid (VFA) accumulation. Methane production was linked with high relative activity and abundance of syntrophic fatty-acid oxidizers alongside hydrogenotrophic methanogens, signaling the importance of interspecies interactions in AD. Specifically, relative activity of *Syntrophomonas* was significantly correlated with methane production. Further, methane production increased over subsequent runs along with methyl coenzyme M reductase (*mcrA)* gene expression, a functional gene in methanogens, suggesting temporal adaptation of the microbial community to co-digestion substrate mixtures. The study demonstrated the benefits of co-digestion in terms of performance enhancement and enrichment of key active microbial populations.

1. Introduction

Anaerobic digestion (AD) of sludge generated during wastewater treatment recovers energy in the form of methane-rich biogas and reduces sludge volume, lessening further treatment and disposal. However, AD requires long retention times and can be sensitive to feed and operational conditions, particularly high free ammonia concentration, relative to aerobic processes (Duan et al., 2012; Li et al., 2011). One option to enhance the performance of AD is to improve biogas production via co-digestion of multiple substrates (e.g., food waste (FW) or fats, oils, and grease (FOG) along with primary and waste activated sludges). Co-digestion can increase the organic loading rate (OLR) but also helps dilute concentrations of potentially toxic compounds, synergistically improve microbial activity, and enhance the nutrient balance (Dai et al., 2013).

FW is a major component of the organic fraction of municipal solid waste (OFMSW), comprising up to 19% of landfill solid waste disposal (Kong et al., 2012). An estimated 4 million dry metric tons per year of landfilled food and processing residuals could potentially generate 248 MWe in an energy recovery process such as AD (Matteson and Jenkins, 2007). In response, California has introduced new legislation, AB1826, that requires the diversion of organic waste from landfills for commercial FW generators thus making AD and composting the leading treatment options (Platt et al., 2014). Under the California law, the minimum threshold of

* Corresponding author.
E-mail address: smithada@usc.edu (A.L. Smith).

http://dx.doi.org/10.1016/j.watres.2017.06.065
0043-1354/

organic waste generation by businesses will decrease over time, resulting in a greater proportion of the commercial sector needing to comply. Other states (e.g., Massachusetts, New York, Connecticut, and Vermont) have instated similar FW diversion regulations (Leibrock, 2017). Permitting composting facilities within dense cities, such as Los Angeles, is challenging given potential odor concerns and large land requirements. Locating compositing facilities outside of large cities is also problematic, as transport distances result in environmental impacts that could potentially outweigh the benefits of landfill diversion altogether. We have documented via life cycle assessment that food waste composting has significant environmental impacts, particularly with regards to eutrophication and respiratory impacts, relative to food waste co-digestion (Becker et al., 2017). Therefore, it is anticipated that AD will play a major role in FW management in the near future.

FOG is a lipid rich waste material that originates from cooking and food processing related industries, such as slaughterhouses and dairy farms (Alqaralleh et al., 2016). Due to the negative impacts of FOG in sewer systems (e.g., formation of hardened deposits that reduce conveyance capacity), grease traps and grease interceptors are placed in collection systems to remove FOG from waste streams (Long et al., 2012). Conventionally, the collected FOG is landfilled; however, newer disposal methods such as AD are becoming more attractive to recover energy and reduce environmental impacts related to disposal (Alqaralleh et al., 2016). In addition, co-digestion of FOG with domestic wastewater sludges has shown a significant increase in biogas production (Long et al., 2012). One concern is that key microbial populations such as acetogens and methanogens could be inhibited by high levels of FOG (Long et al., 2012). Accumulation of long chain fatty acids (LCFA) are thought to damage cell membranes, reduce nutrient transport, and decrease cell permeability affecting the cell's ability to regulate pH (Long et al., 2012; Palatsi et al., 2010; Sousa et al., 2013). Another concern in co-digestion of high strength organics alongside domestic wastewater sludges is the fluctuating characteristics of these substrates and the potential impacts on populations susceptible to toxins, such as methanogens (Karakashev et al., 2005). Therefore, it is crucial to understand how co-digestion affects the AD microbiome to prevent full-scale performance upsets.

The present study was motivated by an initial full-scale test by LA Sanitation's Hyperion Wastewater Treatment Plant (WWTP) in which an increase in biogas production was observed when FW and vegetable cooking oil (VCO) were co-digested with primary sludge (PS) and thickened waste activated sludge (TWAS) relative to digesters receiving only PS and TWAS (Amha et al., 2015a). Co-digestion of VCO at 2% volatile solids loading (VSL) and food waste at 5% VSL led to a 10–15% increase in biogas production, while co-digestion of either substrate alone at the same VSL produced a nominal 0% increase in biogas production (Amha et al., 2015a). In addition, a separate experiment showed that FOG addition at 15% VSL led to a 30% increase in biogas production compared to a control digester only fed with PS and TWAS (Amha et al., 2015a). In the present study, bench-scale respirometry was used as a more controlled approach to confirm full-scale observations by evaluating a range of substrate mixtures and loading rates. Other bench-scale studies have previously demonstrated performance-based benefits of FW co-digestion (Koch et al., 2015, 2016; Li et al., 2016), FOG co-digestion (Davidsson et al., 2008; Girault et al., 2012; Kabouris et al., 2009; Noutsopoulos et al., 2013; Wang et al., 2013; Ziels et al., 2016), and simultaneous co-digestion of FW and FOG (Li et al., 2011; Wu et al., 2016; Xu et al., 2015). Few studies have evaluated the impact of co-digestion of FOG on the AD microbiome (Girault et al., 2012; Martín-González et al., 2011; Xu et al., 2015; Yang et al., 2016; Ziels et al., 2015, 2016). The majority of these studies were done at mesophilic temperatures (Davidsson et al., 2008; Koch et al., 2015; Li et al., 2011, 2016; Wang et al., 2013; Xu et al., 2015; Yang et al., 2016; Ziels et al., 2016), with only a few studies done at thermophilic temperatures (Alqaralleh et al., 2016; Kabouris et al., 2009; Li et al., 2015; Martín-González et al., 2011; Zhu et al., 2015).

Recent advances in molecular biological tools have led to an influx in research evaluating microbial community structure and activity on AD performance. AD is a relatively complex chain of microbial processes including hydrolysis, fermentation, acetogenesis, and methanogenesis, where methanogenic archaea are divided into acetoclastic and hydrogenotrophic depending on electron donor. A few studies have evaluated AD community dynamics during co-digestion of FOG and/or FW using traditional molecular methods (Hatamoto et al., 2007; Martín-González et al., 2011; Palatsi et al., 2010) and high-throughput DNA-based sequencing (Li et al., 2016; Sundberg et al., 2013; Yang et al., 2016; Ziels et al., 2016). However, DNA-based sequencing approaches detect inactive cells (Amha et al., 2015b) and can be inaccurate during perturbation in AD (De Vrieze et al., 2016), making it difficult to link function and microbial community structure. Therefore, the current study aims to understand how co-digestion of FW and FOG influences microbial community structure and activity using both DNA- and RNA-based Illumina sequencing of the 16S rRNA gene and 16S rRNA, respectively, and reverse transcription quantitative PCR (RT-qPCR) of the methyl coenzyme M reductase (*mcrA*) gene in methanogens. To our knowledge, this is the first study to use both DNA and RNA-based Illumina sequencing to study co-digestion of FW and FOG. These molecular tools were employed across three sequential bench-scale respirometery runs conducted under varying substrate mixtures at thermophilic conditions and during two additional runs evaluating FOG inhibition at high VSLs. Outcomes of the research are expected to inform decisions at the full-scale regarding substrate ratios and maximum advisable OLRs.

2. Materials and methods

2.1. Sample collection and chemical assays

PS, TWAS, FOG, and seed (biomass from a full-scale thermophilic AD) samples were collected from Hyperion WWTP (Los Angeles, CA). FW samples were obtained from Divert, Inc. (Compton, CA). Biomass samples for DNA and RNA analyses were processed onsite during sample collection by centrifuging and decanting the supernatant to pelletize biomass in 2 mL centrifuge tubes. For RNA preservation, biomass was stabilized using DNA/RNA shield (Zymo Research, Irvine, CA). Preserved biomass samples were transported on ice to the University of Southern California (USC) after which they were stored at −80 °C until further processing.

2.2. Bench-scale anaerobic respirometry

Bench-scale respirometry experiments were conducted using a MPA-200 Methane Potential Analyzer (Challenge Technology, Springdale, AR) containing 15 replicate 500 mL continuously-stirred glass reactor vessels. Three sequential batch runs (Runs 1–3) were conducted containing PS, TWAS, FOG, and FW according to Table 1 (% v/v) at a TVS concentration of approximately 10 g/L. The effective liquid volume was maintained at 400 mL by adding PBS buffer (137 mM NaCl, 2.7 mM KCl, 10 mM Na_2HPO_4, and 2 mM KH_2PO_4) as necessary. For Run 1, all reactor vessels were inoculated with 200 mL of seed from a full-scale thermophilic AD at Hyperion WWTP. However, for the subsequent two runs (Run 2 and 3), biomass from the preceding run fed with all substrates (PS, TWAS, FOG, and FW) was used as seed to evaluate if microbial community adaptation was beneficial to performance in other substrate

mixtures considered. Although not reseeding in this way may have led to more dramatic changes in microbial community structure and relative activity, this approach enabled evaluation of each run independent of differences in inoculum. The control vessels were only inoculated with 200 mL of seed and PBS buffer to attain the effective liquid volume. Therefore, these vessels did not contain other substrates (Table 1). Prior to startup, the vessels were purged with nitrogen gas for 10 min to create anaerobic conditions. Subsequently, the vessels were partially submerged in a recirculating water bath to maintain a thermophilic temperature of 50 °C to replicate conditions of the full-scale AD at Hyperion WWTP. Vessels were continuously stirred at 250 rpm using magnetic stir bars. Biogas composition, chemical assay, and lag-phase (using non-linear regression) were analyzed as described in Appendix S1.

Two additional runs (Run 4 and 5) were conducted to assess potential inhibition during high FOG addition. For Run 4, 30% and 60% FOG TVS addition was evaluated with and without 10% FW TVS, whereas in Run 5, 30%, 40%, 50%, and 60% FOG TVS addition were evaluated with 10% FW TVS (Table 1) and the balance from PS and TWAS (i.e., identical TVS addition to all vessels). For Run 4, sludge from a full-scale thermophilic AD at Hyperion WWTP was used as seed, whereas for Run 5, biomass from Run 4 30% FOG+FW condition was used as seed for all vessels. In both runs, 200 mL of seed was used to inoculate the vessels and all conditions were run in triplicates. As in the first phase of the study, the vessels were kept at 50 °C and continuously stirred at 250 rpm.

2.3. Nucleic acids extraction and cDNA synthesis

Biomass samples were taken at the beginning and end of each run, centrifuged at 5000×*g* for 5 min at 4 °C, decanted, and preserved at −80 °C until further processing. DNA and RNA extraction from preserved biomass was performed using Maxwell extraction kits (Promega, Madison, WI), as further described in Appendix S1. For the RNA extracts, an additional DNase treatment was conducted using DNA-free™ DNA Removal Kit (Invitrogen, Carlsbad, CA) to remove DNA contamination. Reverse transcription to generate single-stranded complementary DNA (cDNA) from RNA extracts was performed using GoScript™ Reverse Transcription System according to manufacturer's instructions (Promega, Madison, WI). 100 ng of RNA was taken from each sample for cDNA synthesis.

Table 1
Substrate volatile solid loading for bench-scale anaerobic respirometry. Each condition was run in triplicate vessels containing 10 g L^{-1} of TVS.

	% Volatile solid loading			
	PS	WAS	FW	FOG
Run 1–3				
Control (1–3)	0	0	0	0
PS+TWAS (4–6)	50	50	0	0
PS+TWAS+FOG (7–9)	45	45	0	10
PS+TWAS+FW (10–12)	45	45	10	0
PS+TWAS+FOG+FW (13–15)	40	40	10	10
Run 4 (FOG Inhibition)				
Control (1–3)	0	0	0	0
30%FOG+FW (4–6)	30	30	10	30
30%FOG (7–9)	35	35	0	30
60%FOG+FW (10–12)	15	15	10	60
60%FOG (13–15)	20	20	0	60
Run 5 (FOG Inhibition)				
Control (1–3)	0	0	0	0
30%FOG+FW (4–6)	30	30	10	30
40%FOG+FW (7–9)	35	35	0	30
50%FOG+FW (10–12)	15	15	10	60
60%FOG+FW (13–15)	20	20	0	60

2.4. PCR and sequencing

Due to the potential for differences in microbial community structure and activity within replicate vessels under the same substrate mixtures, triplicate DNA and RNA samples for Run 1, and triplicate DNA and duplicate RNA samples for Run 3 were taken for analysis (Table S1). PCR for 16S rRNA gene sequencing and 16 rRNA (cDNA transcript) sequencing was conducted using a universal 16S rRNA gene primer set targeting the V4 region (Appendix S1). The sequencing results were analyzed using mothur (Schloss et al., 2009) according to the Schloss MiSeq SOP. Resulting sequences from the first phase of the study (Run 1–3) and the FOG inhibition study (Run 4–5) were analyzed separately, as described in detail in Appendix S1. We define “relative abundance” as the percentage of 16S rRNA gene sequences for a given population out of the total 16S rRNA gene sequences and define “relative activity” as the percentage of 16S rRNA sequences for a given population out of the total 16S rRNA sequences. Spearman's rank was used for non-parametric analysis to correlate the microbial community profile with methane production using MaxStat 3.6 (Germany). Significant correlation was defined as $p < 0.05$. All raw sequences form this study are available in NCBI's Sequence Read Archive (SRA) database (Leinonen et al., 2011) (SRA Study SRP102955).

2.5. Reverse transcription-quantitative PCR (RT-qPCR)

The 16S rRNA and *mcrA* transcripts were quantified using RT-qPCR. Positive controls for 16S rRNA and *mcrA* were isolated from a pool of 10 cDNA samples used in the study and pooled by equal mass. PCR to prepare the RT-qPCR standards was performed as previously described (Smith et al., 2015) (Appendix S1). Genomic DNA of *Thermus thermophilus* isolated from pure culture (American Type Culture Collection (ATCC) 27634) was used as a negative control and ultra-pure DNase/RNase free water was used as a no-template control. Melt curve analysis was conducted to check for specificity of amplifications. The R^2 value for the 16S rRNA standard curve was 1.00 with an average efficiency of 78.0%. The R^2 value for the *mcrA* standard curve was also 1.00 and the average efficiency was 84.0%.

2.6. Reagent controls

To evaluate potential contamination from extraction kits and reagents, sequencing was performed on serial dilutions of a pure culture using a similar approach to Salter et al., (2014). *Thermus thermophilus* (ATCC 27634) was used as an internal standard to make six, ten-fold serial dilutions, which were taken for DNA extraction and subsequent sequencing targeting the 16S rRNA gene. In addition, qPCR was conducted on DNA and reverse transcribed cDNA from RNA extracts of the different dilutions of *Thermus thermophilus* to quantify the observed contamination. Further details on methodology and results from these observations can be found in the SI.

3. Results and discussion

3.1. Co-digestion of FOG and FW reproducibly increased methane production

Bench-scale respirometery of the substrate mixtures indicated reproducible improvement in methane production, with Run 3 PS+TWAS+FOG+FW and PS+TWAS+FOG exhibiting 26.0 ± 8.1% and 21.1 ± 6.6% increase in methane production relative to PS+TWAS, respectively. While PS+TWAS+FOG and PS+TWAS+FOG+FW also showed an increase in methane production in the preceding runs

(Fig. 1), PS+TWAS+FW only showed an increase in methane production relative to PS+TWAS by Run 3 (18.4 ± 3.2%). In Run 3, mean methane production for PS+TWAS+FW, PS+TWAS+FOG, and PS+TWAS+FOG+FW was significantly greater than PS+TWAS (unpaired one-tail *t*-test, $p < 0.05$). The differences in mean methane production were 19.1 mL CH_4 g TVS^{-1} ($p = 0.0063$) for PS+TWAS+FW, 22.1 mL CH_4 g TVS^{-1} ($p = 0.0145$) for PS+TWAS+FOG, and 27.0 mL CH_4 g TVS^{-1} ($p = 0.0206$) for PS+TWAS+FOG+FW. Therefore, FOG addition was associated with greater improvement in methane production than FW addition, confirming full-scale observations at Hyperion WWTP (Amha et al., 2015a). Full-scale experiments observed a 30% increase in digester gas production during 15% VSL FOG co-digestion compared to a control digester fed with only PS and TWAS. Conversely, co-digestion of FW at 10% VSL only increased digester gas production by 10% (Amha et al., 2015a). Bench-scale PS+TWAS+FW showed a higher improvement in performance in Run 3 than was obtained at the full scale (Amha et al., 2015a), but overall PS+TWAS+FW performance was inconsistent with insignificant performance improvements in Run 1 and 2. The inconsistency observed may have resulted from fluctuating FW characteristics, which is a potential risk in full-scale facilities, particularly when FW comprises a large fraction of the OLR. Methane production increased in subsequent runs across all substrate mixtures, with the highest production observed in Run 3 consistently (Fig. 1). For example, mean methane production for PS+TWAS+FOG+FW increased by 38.8 mL CH_4 g TVS^{-1} ($p = 0.0125$) in Run 3 relative to Run 1. It is important to note that all vessels in Run 2 and 3 were seeded with the same inoculum, biomass from the preceding run from the PS+TWAS+FOG+FW substrate mixture. Therefore, microbial community adaptation to the co-digestion substrate mixture improved performance in Run 2 and 3 across all substrate mixtures (vessels) suggesting that temporary co-digestion can be beneficial in improving process performance.

Non-linear regression analysis of biogas production indicated a decrease in lag phase (λ) from Run 1 to 3 for substrate mixtures containing FOG (Table 2, Fig. S3). The lowest lag phase was observed for PS+TWAS, ranging from 40.6 to 62.3 h, of all substrate mixtures, followed by PS+TWAS+FW ranging from 53.0 to 88.6 h. The largest decrease in lag phase was observed for PS+TWAS+FOG, which decreased from 118 ± 2 h in Run 1 to 46.3 ± 12.5 h in Run 3. A more moderate decrease in lag phase was observed for PS+TWAS+FOG+FW, which decreased from 114 ± 10 h in Run 1 to 85.0 ± 23.1 h in Run 3. Conversely, PS+TWAS+FW showed an increase in lag phase, comparing Run 3 and Run 1. These results suggest that addition of FOG increased lag phase initially but was significantly diminished in subsequent runs due to adaptation of the microbial community. Acclimation of the microbial community to FOG has been shown to shorten lag phase and increase methane activity (Silva et al., 2014; Silvestre et al., 2011; Ziels et al., 2016), corroborating our observed significant lag phase reduction with the reseeding of acclimated biomass from previous runs.

Run 3 PS+TWAS+FOG+FW showed the highest TVS reduction (41.3 ± 7.1%) and lowest free ammonia concentration (24.9 ± 1.2 mg NH_3 L^{-1}), correlating well with the high methane production observed (Table 3). TVS reduction ranged from 35.7 to 41.3% in Run 3 for the various substrate mixtures. Free ammonia concentrations ranged from 24.9 to 38.9 mg NH_3 L^{-1}, well under the inhibitory concentration of 100–150 mg NH_3 L^{-1} for AD communities (Hansen et al., 1998). Sulfate removal ranged from 64 to 67% under all substrate mixtures and was thus not influenced by co-digestion. Low concentrations of VFAs were observed at the end of each run for most vessels. However, PS+TWAS+FW vessels contained elevated propionate concentrations at the end of Run 3.

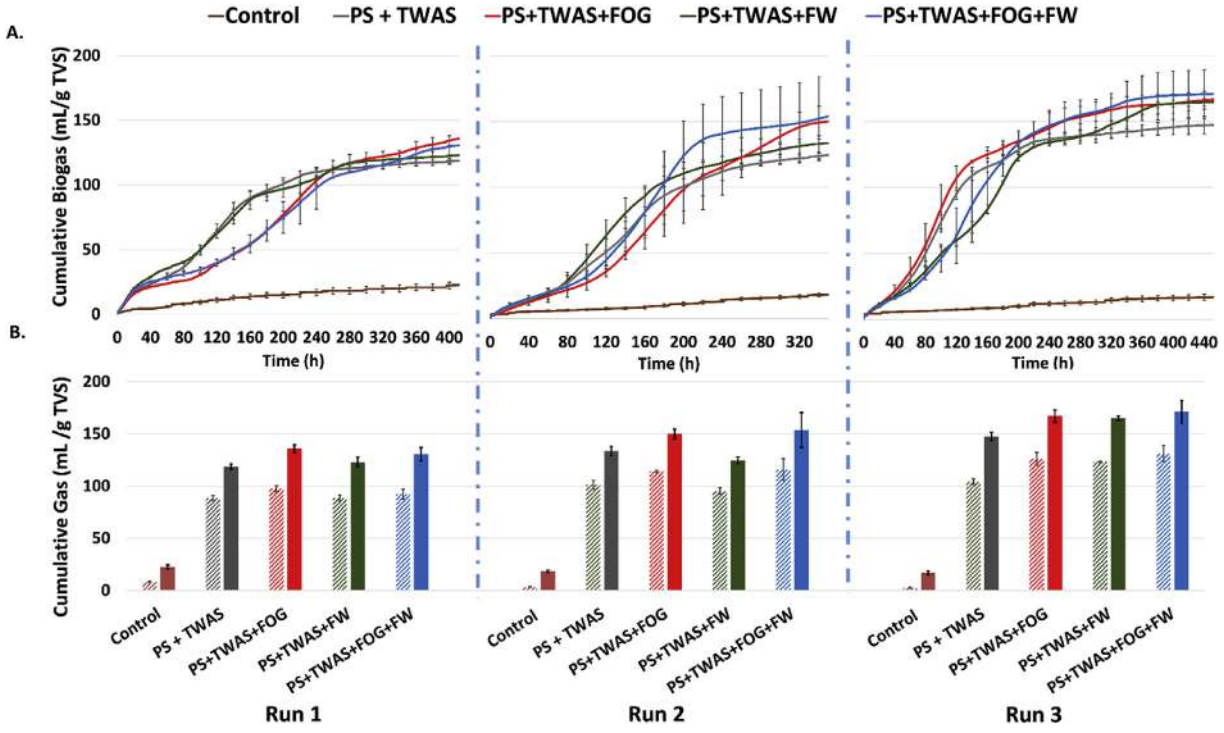

Fig. 1. **(A)** Cumulative biogas production normalized to initial organic loading in mL g TVS^{-1} for Run 1, Run 2, and Run 3. The error bars indicate the standard deviation every 20 h for triplicate vessels. **(B)** Cumulative biogas (solid fill) and methane (pattern fill) for the substrate mixtures, normalized to initial organic loading in mL g TVS^{-1}. Error bars indicate the combined standard deviation of cumulative biogas/methane production and initial organic loading TVS measurement for triplicate vessels. Due to experimental error, one of the triplicate vessels for the following substrate mixtures and runs were excluded from the mean analysis and standard deviation: PS+TWAS+FOG (in Run 1), PS+TWAS+FW (in Run 3), and PS+TWAS+FOG+FW (in Run 3). Therefore, each bar represents the mean of only two vessels for these substrate mixtures and runs.

Table 2
Non-linear regression analysis on all substrate mixtures in Run 1, 2, and 3.

	A (mL g TVS^{-1})	λ (h)	μ_m (mL g TVS^{-1} h)	R^2
Run 1				
PS+TWAS	114 ± 2	55.4 ± 3.7	1.09 ± 0.12	0.980 ± 0.001
PS+TWAS+FOG	123 ± 3	118 ± 2	1.32 ± 0.001	0.943 ± 0.004
PS+TWAS+FW	115 ± 7	53.0 ± 3.2	1.10 ± 0.07	0.943 ± 0.012
PS+TWAS+FOG+FW	116 ± 12	114 ± 10	1.30 ± 0.03	0.909 ± 0.045
Run 2				
PS+TWAS	127 ± 4	62.3 ± 16.5	1.15 ± 0.16	0.989 ± 0.007
PS+TWAS+FOG	146 ± 16	115 ± 10	1.41 ± 0.32	0.971 ± 0.023
PS+TWAS+FW	121 ± 2	74.9 ± 16.6	1.13 ± 0.11	0.976 ± 0.012
PS+TWAS+FOG+FW	148 ± 32	103 ± 9	1.66 ± 0.05	0.980 ± 0.016
Run 3				
PS+TWAS	142 ± 4	40.6 ± 4.3	1.27 ± 0.01	0.993 ± 0.004
PS+TWAS+FOG	156 ± 11	46.3 ± 12.5	1.64 ± 0.04	0.967 ± 0.031
PS+TWAS+FW	139 ± 22	88.6 ± 13.0	1.45 ± 0.25	0.952 ± 0.014
PS+TWAS+FOG+FW	142 ± 38	85.0 ± 23.1	1.53 ± 0.25	0.965 ± 0.030

3.2. Syntrophic fatty-acid oxidizers were critical to increase methane production

RNA-based sequencing was more sensitive than DNA-based sequencing in evaluating microbial population dynamics across various substrate mixtures. For example, 16S rRNA sequence data indicated that *Coprothermobacter* and *Thermotogales* were relatively inactive at 50% FOG and 60% FOG during the FOG inhibition study (Run 5). However, 16S rRNA gene sequence data showed only a minor reduction in their relative abundance. Further, *Mycobacterium* had relatively high abundance in all substrate mixtures based on 16S rRNA gene sequence data (1.61–3.99% relative abundance at end of Run 3; Fig. S7), but they were not detected in 16S rRNA sequencing, suggesting they were inactive (Fig. 2). *Mycobacterium* are known to have DNA that persists in the environment (Kumaraswamy et al., 2014). Therefore, their detection with DNA sequencing could be due to inactive cells, highlighting the main shortcoming of DNA-based analyses. Similar observations have been reported in a previous study under inhibitory conditions (De Vrieze et al., 2016). Based on these concerns, more emphasis was given to the RNA-based sequencing in the following discussion on the microbial community. DNA-based sequencing results can be found in Appendix S2 (Figs. S6–S8 and S14–S16).

The Spearman rank correlation analysis showed significant ($p < 0.05$) but weak correlation ($R = 0.475$, $p = 0.0189$) between methane production and total methanogenic relative activity (Table S2), which was obtained by summing the relative activity of methanogens identified to the genus-level for each substrate mixture. The relative activity of methanogens increased from Run 1 to Run 3 in all substrate mixtures except for PS+TWAS (Fig. 3A). The increase was highest in PS+TWAS+FOG+FW, where the relative activity increased from 0.410% at the end of Run 1 to 0.873% at the end of Run 3. PS+TWAS+FOG+FW also showed the highest methane production increase with subsequent runs (Fig. 1). PS+TWAS exhibited a higher relative activity of methanogens in Run 1 and 2 than any other substrate mixture, but this likely resulted from an increase in hydrolytic bacteria and fermenter relative activity during co-digestion in all other substrate mixtures rather than an actual decrease in methanogenic relative activity. The biogas production data supports this notion. Methanogens also exhibited high relative activity in the control vessels, likely stemming from relative activity decreases of other populations. According to Spearman rank, the *mcrA*/16S rRNA ratio was not significantly correlated with methane production ($p = 0.6743$). Similarly, a previous study reported that *mcrA* expression did not correlate with methane production (Morris et al., 2014). Nonetheless, considering the four different substrate mixtures, the ratio of *mcrA* transcripts to 16S rRNA copies increased substantially with increasing run (Fig. 4) and with increasing methane production except for PS+TWAS, where Run 2 ratios exceeded Run 3. In the control where methane production was lowest in all runs, *mcrA* gene expression was high, likely due to decreased relative activity of other populations such as hydrolytic bacteria and fermenters that were not receiving substrates. Methanogenic relative activity was thus likely artificially inflated due to endogenous decay. These observations highlight the need for absolute abundance/activity data to more accurately monitor engineered systems, as discussed in a recent study that concluded that increases in relative abundance do not necessarily reflect increases in absolute abundance/outgrowth of taxa (Props et al., 2016). It is also important to note some of the shortcomings of using 16S rRNA genes and 16S rRNA to infer microbial community structure and relative activity, respectively. Analysis of 16S rRNA is not linked with a specific cellular function and does not always relate with activity (Blazewicz et al., 2013). In addition, the relationship between 16S rRNA copies and growth rate can differ between populations (Blazewicz et al., 2013). Further, using 16S rRNA genes to infer community structure is complicated by 16S rRNA operon numbers varying from 1 to 15 per genome (Klappenbach et al., 2000), resulting in potential under- or over-representation of certain taxa.

Table 3
TVS removal, free ammonia concentration, pH, VFA concentration, sulfate concentration, and sulfate reduction for end of Run 3. The detection limit for the IC analyses was 10 mg L^{-1}.

	TVS removal (%)	Free ammonia (mg L^{-1})	pH	Acetate (mg L^{-1})	Propionate (mg L^{-1})	Butyrate (mg L^{-1})	Formate (mg L^{-1})	Valerate (mg L^{-1})	Sulfate (mg L^{-1})	Sulfate reduction (%)
Control	7.80 ± 8.1	228 ± 14	8.26 ± 0.01	84.7 ± 26.5	14.9 ± 0.3	<10	<10	<10	21.0 ± 0.4	81.7 ± 2.5
PS+TWAS	35.7 ± 2.3	38.9 ± 2.4	7.12 ± 0.03	16.1 ± 0.4	<10	<10	<10	<10	29.5 ± 0.3	64.3 ± 1.2
PS+TWAS+FOG	38.0 ± 0.6	35.7 ± 4.4	7.09 ± 0.05	36.7 ± 0.3	47.7 ± 0.2	<10	<10	<10	57.5 ± 1.5	65.9 ± 0.1
PS+TWAS+FW	34.1 ± 0.9	33.6 ± 0.2	7.05 ± 0.01	29.7 ± 0.1	179 ± 0.8	17.5 ± 0.0	<10	73.8 ± 0.7	29.0 ± 0.2	67.4 ± 1.2
PS+TWAS+FOG+FW	41.3 ± 7.1	24.9 ± 1.2	6.94 ± 0.02	25.6 ± 0.3	<10	94.3 ± 0.6	<10	<10	33.6 ± 0.1	64.1 ± 0.9

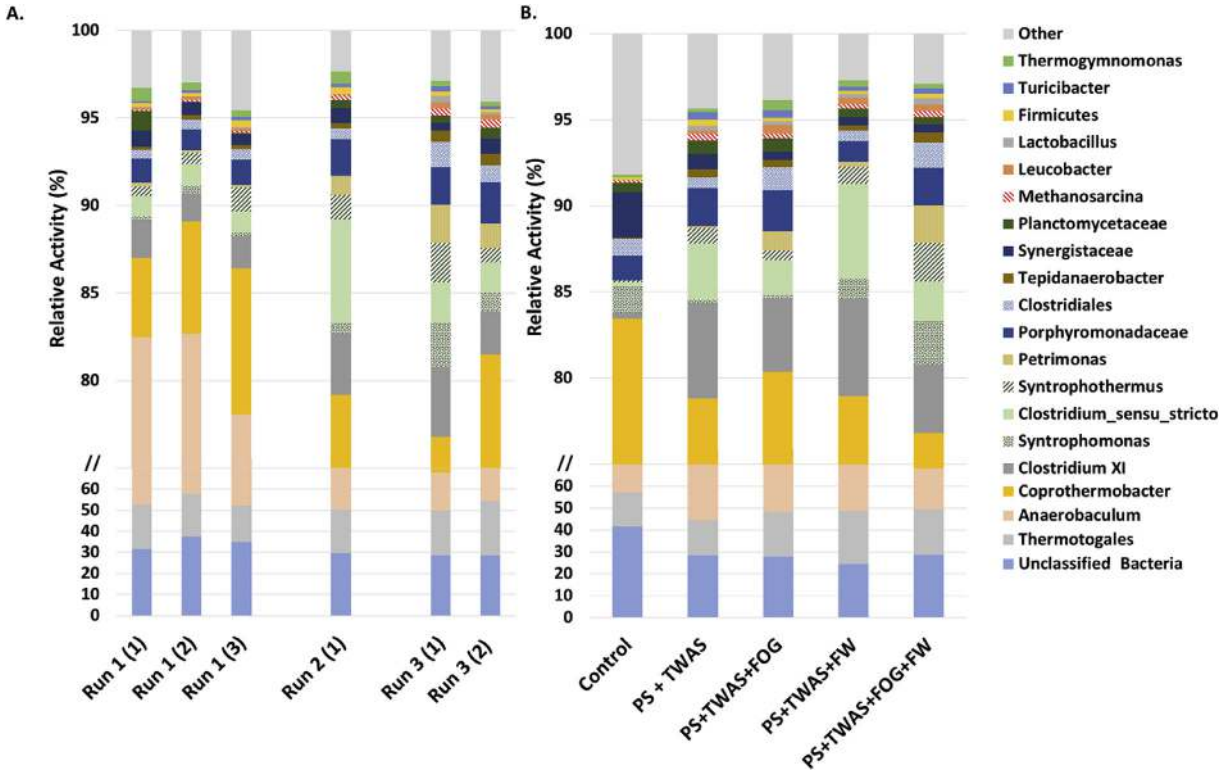

Fig. 2. **(A)** Relative activity based on 16S rRNA sequencing identified at the genus level where possible for PS+TWAS+FOG+FW for Run 1, Run 2, and Run 3. For Run 1 and Run 3, triplicate and duplicate samples are shown, respectively, to represent methodological precision. **(B)** Relative activity in at the end of Run 3 for the different substrate mixtures. All data are expressed as a percentage normalized using total 16S rRNA sequences (*Bacteria* and *Archaea*). A y-axis break was used to accentuate differences in lower activity populations.

The relative activity of two methanogenic genera, *Methanoculleus* ($R = 0.7488$, $p < 0.001$) and *Methanosarcina* ($R = 0.521$, $p = 0.009$), showed significant positive correlation with methane production (Table S2). *Methanosarcina* spp. showed the highest relative activity (Fig. 3A) in most samples. *Methanosarcina* are mixotrophic methanogens that are able to metabolize hydrogen, acetate, and C1 compounds (Mladenovska and Ahring, 1997; Welander and Metcalf, 2005), which can be considered an advantage over other methanogens by providing metabolic flexibility. In addition, obligatory hydrogenotrophic methanogens such as *Methanobacterium, Methanobrevibacter, Methanosphaera,* and *Methanothermobacter* were detected. *Methanosaeta* spp., obligate acetoclastic methanogens, were only detected in the control in Run 1 (0.013%) and PS+TWAS+FOG+FW in Run 3 (0.013%). *Methanosaeta* are known to have higher substrate affinity for acetate and lower growth rate than *Methanosarcina*, which means they typically outcompete *Methanosarcina* at low acetate concentrations (Conklin et al., 2006). The extremely low presence of *Methanosaeta* spp. suggests that acetate oxidation was performed exclusively by *Methanosarcina* spp. or via other metabolic processes (e.g., syntrophic acetate oxidation or sulfate reduction). Notably, acetate did not accumulate in any of the substrate mixtures (Table 3). Further, sulfate concentrations were relatively low in all of the substrate mixtures. For example, the influent sulfate concentration for the substrate mixtures averaged only 87.0 ± 5.2 mg L^{-1} for Run 3. Thus, there was limited enrichment of sulfate reducing bacteria, accounting for less than 0.1% of the relative activity across all substrate mixtures at the end of Run 3.

The absence of *Methanosaeta* spp. and low presence of sulfate reducing bacteria could indicate that syntrophic acetate oxidizers such as *Thermacetogenium*, *Syntrophaceticus,* and *Tepidanaerobacter* (Westerholm et al., 2011), played a significant role in acetate oxidation. For example, *Tepidanaerobacter* showed relative activity of 1.05% and 1.20% in PS+TWAS+FOG and PS+TWAS+FW, respectively (Fig. 3B). *Tepidanaerobacter* ($R = 0.419$, $p = 0.042$) and *Syntrophaceticus* ($R = 0.424$, $p = 0.039$) relative activity was also significantly correlated with methane production. In addition, there was an enrichment of all three syntrophic acetate oxidizers over sequential runs (Fig. S9). Unclassified sequences belonging to the family *Thermoanaerobacteraceae* showed a relative activity of 0.026–0.212% in the various substrate mixtures. *Thermoanaerobacteraceae* includes known syntrophic acetate oxidizers, such as *Thermacetogenium* and *Tepidanaerobacter* (Mosbæk et al., 2016), but it is difficult to conclude the role of these groups at this phylogenetic resolution. Syntrophic acetate oxidizers have a thermodynamic advantage at higher temperatures (Hao et al., 2010) and the thermophilic temperature in this study could have aided enrichment of these groups over time. It should be noted that there are few known syntrophic acetate oxidizers (i.e., *Syntrophaceticus* spp., *Thermacetogenium phaeum*, *Thermotoga lettingae*, *Tepidanaerobacter acetatoxydans*, and *Clostridium ultunense* (Westerholm et al., 2011)). Recent studies have demonstrated that cluster II *Spirochaetes* could perform syntrophic acetate oxidation with hydrogenotrophic methanogens (Lee et al., 2015), but OTUs classifying as *Spirochaetes* comprised less than 0.1% relative activity for most samples here. We did detect high relative activity of OTUs belonging to *Clostridium*, however, no OTUs classified within *Clostridium XII* in Run 1–3, which is the cluster that includes the known syntrophic acetate oxidizer *Clostridium ultunense* (Schnürer et al., 1996). Syntrophic acetate oxidation is likely performed by yet to be described microbial populations rather than known cultures of syntrophic acetate oxidizers (Werner et al., 2014). Therefore, these undescribed

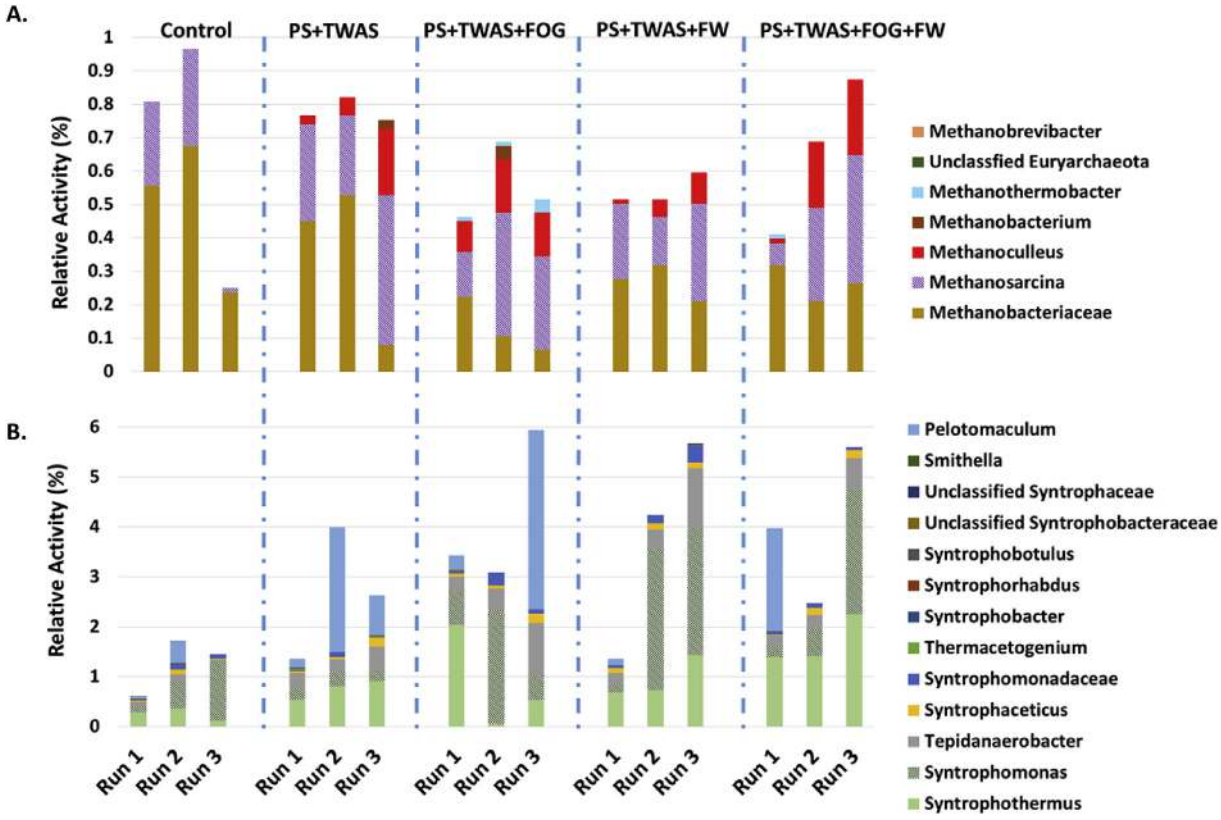

Fig. 3. **(A)** Relative activity of methanogens identified at the genus level where possible based on 16S rRNA sequencing and **(B)** relative activity of syntrophic fatty-acid oxidizers identified at the genus level where possible using 16S rRNA sequencing. Results are expressed as a percentage normalized using total of 16S rRNA sequences (*Bacteria* and *Archaea*). Truncated y-axes (0–1% and 0–6% on A and B, respectively) are shown to accentuate differences in abundance.

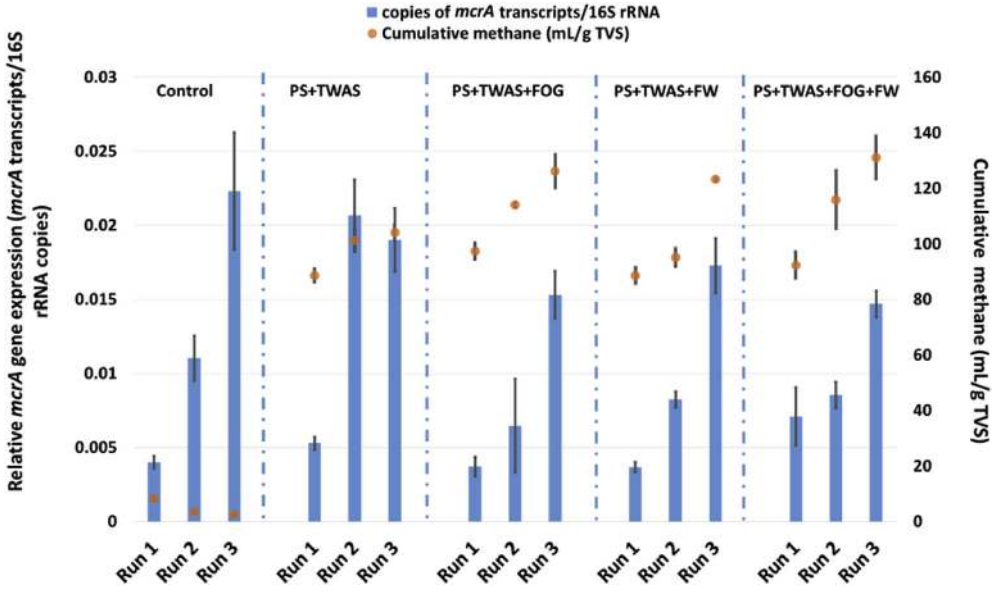

Fig. 4. Relative expression of *mcrA* in all substrate mixtures for Run 1–3. Copies of *mcrA* transcripts were normalized to total 16S rRNA copies. Error bars for *mcrA* expression represent the standard deviation of the ratio of triplicate RT-qPCR reactions. Error bars for cumulative methane production (secondary y-axis) represent the standard deviation for triplicate vessels.

populations likely play a significant role in acetate consumption here and in other AD systems. Further research is needed using DNA/RNA-stable isotope probing with ^{13}C -labeled acetate to identify and better understand these key populations.

The high relative activity of hydrogenotrophic methanogens in all substrate mixtures and runs indicated the importance of syntrophy in improving biogas production. Oxidation of reduced compounds, such as fatty acids, by secondary fermenting bacteria is thermodynamically

unfavorable when not coupled with a hydrogen-consuming syntrophic partner to keep hydrogen partial pressure low (Hattori, 2008). Our sequencing results reinforce the importance of this interspecies interaction. Plotting methane production vs. total relative activity of syntrophic fatty-acid oxidizers and methanogens for all substrate mixtures (Fig. S10) gave a visual representation of the increased methane production with increasing relative activity of these groups. Further, syntrophic fatty-acid oxidizers were enriched over time in PS+TWAS+FOG+FW, although relative activity of specific syntrophs shifted in sequential runs. For example, *Pelotomaculum* accounted for the highest relative activity in Run 1 PS+TWAS+FOG+FW but this population was completely replaced by *Syntrophothermus* and *Syntrophomonas* by Run 3. *Syntrophomonas* are syntrophic fatty acid β-oxidizing bacteria that are able to oxidize LCFA, and have been shown to be highly active during FOG co-digestion (Ziels et al., 2016). *Pelotomaculum* remained dominant in PS+TWAS across all runs. In PS+TWAS+FOG, these populations resurfaced in Run 3 after disappearing in Run 2. *Tepidanaerobacter* significantly increased in relative activity in all substrate mixtures other than the control from Run 1 to Run 3 (Fig. 3B). Overall, the observed increase in relative activity of hydrogenotrophic methanogens and syntrophic fatty-acid oxidizers with increasing biogas production highlights the significance of syntrophy in co-digestion. Similar observations have been reported by other researchers (Ziels et al., 2015, 2016). For example, a study on the impact of high FOG addition in a mesophilic, semi-continuous anaerobic digester found an increase of hydrogenotrophic methanogen *Methanospirillum* from a relative abundance of 1.3%–34% over 138 days along with an increase in relative abundance of *Syntrophomonas* (Ziels et al., 2016).

The observed increase in the sum of the relative activity of *Syntrophomonas* and *Syntrophothermus* in PS+TWAS+FOG+FW relative to PS+TWAS+FOG and PS+TWAS+FW suggests that these populations of syntrophic fatty-acid oxidizers (Narihiro et al., 2015; Sekiguchi et al., 2000; Sousa et al., 2009) may be key to the increase in biogas production observed at the bench and full scale. Relative activity data for Run 3 showed that *Syntrophomonas* and *Syntrophothermus* were not significant in PS+TWAS, each comprising less than 1.00% of the relative activity (Fig. 4B). PS+TWAS+FW showed substantially higher relative activity of these key populations, accounting for 2.53% and 1.44% of the relative activity, respectively (Fig. 3B). The enrichment of these populations in PS+TWAS+FW by Run 3 may be the reason for the enhanced performance observed compared to PS+TWAS. In addition, other populations with significant positive correlation with methane production (Table S2) also showed high relative activity in PS+TWAS+FW, such as *Clostridium sensu stricto* ($R = 0.571$, $p = 0.004$), *Clostridium XI* ($R = 0.655$, $p = 0.0005$), and *Tepidanaerobacter* ($R = 0.419$, $p = 0.042$), with relative activity of 5.50%, 5.65%, and 1.20%, respectively (Fig. 2). In PS+TWAS+FOG+FW, *Syntrophomonas* and *Syntrophothermus* were also relatively more active compared to PS+TWAS, comprising 2.51% and 2.25% of the relative activity, respectively. Interestingly, these populations had low relative activity in PS+TWAS+FOG in Run 3. Notably, there was a positive correlation between methane production and total relative activity of syntrophs ($R = 0.475$, $p = 0.0192$) and relative activity of *Syntrophomonas* ($R = 0.406$, $p = 0.0491$) (Table S2). A correlation between performance enhancement and increase in relative abundance of *Syntrophomonas* was also reported previously (Ziels et al., 2016). In addition, a more recent study reported that the kinetics of LCFA degradation rate correlated to the relative abundance of *Syntrophomonas* (Ziels et al., 2017). Diversity analysis using the inverse Simpson metric revealed that the highest diversity was in PS+TWAS+FOG+FW and that diversity increased with sequential runs (Fig. S12). The inverse Simpson metric for PS+TWAS+FOG+FW increased by 38.7% from Run 1 to Run 3 while PS+TWAS+FOG and PS+TWAS+FW showed a more modest temporal increase in diversity. The increase in diversity was largely driven by upper-level fermenters, which remain somewhat poorly described in the AD microbiome and deserve further study.

3.3. High FOG addition resulted in significant decline in performance and inhibited key microbial populations

Run 4 demonstrated that 60% FOG addition was severely inhibitory and FW addition at high FOG only moderately improved performance. A steep decline in methane production occurred at 60% FOG addition (Fig. 5). FW addition increased methane production in the 30% FOG mixtures by 31.0 ± 19.9%, relative to FOG addition without FW. Relative to Run 1 PS+TWAS (Fig. 1), methane production increased by 47.5 ± 9.8% and 12.6 ± 16.0% for 30% FOG+FW and 30% FOG, respectively. The mean methane production compared to Run 1 PS+TWAS increased by 42.1 mL CH_4 g TVS^{-1} ($p = 0.0034$) for the 30% FOG+FW condition, and 11.2 mL CH_4 g TVS^{-1} ($p = 0.24$) for the 30% FOG condition. The increase in mean methane production for the 30% FOG condition compared to Run 1 PS+TWAS was insignificant ($p > 0.05$) due to high variability within the triplicate vessels for the substrate mixture.

For Run 5, 10% FW addition was applied uniformly to 30%, 40%, 50%, and 60% FOG (Table 1), since Run 4 suggested that co-digestion of FW at high FOG addition increased performance. All conditions were seeded with biomass from Run 4 30% FOG+FW. Relative to Run 1 PS+TWAS, methane production was highest at 30% FOG with a 53.3 ± 18.2% increase. Methane production also increased at 40% FOG but by only 27.4 ± 19.6% relative to Run 1 PS+TWAS. At higher FOG loading, methane production decreased relative to Run 1 PS+TWAS by 90.3 ± 1.6% and 94.4 ± 2.3% at 50% and 60% FOG, respectively. The increase in mean methane production for 30% FOG and 40% FOG in Run 5 compared to Run 1 PS+TWAS was 47.2 ($p = 0.02$) and 24.2 ($p = 0.11$) mL CH_4 g TVS^{-1}, respectively. Conversely, the 50% FOG and 60% FOG showed a decrease of 79.9 ($p < 0.0001$) and 83.6 ($p < 0.0001$) mL CH_4 g TVS^{-1}. One of the triplicate vessels for 40% FOG showed an outlier in methane production compared to the other replicates suggesting less stability in performance at this FOG loading. Excluding this outlier vessel, 40% FOG showed similar biogas production to 30% FOG, although at a lower methane content. Both scenarios showed high variability within triplicate vessels and long lag phase (Fig. S13). Due to the long lag phase, Run 5 was conducted for a total of 800 h.

High concentrations of VFAs at 50% and 60% FOG suggested inhibition of methanogens and syntrophic fatty-acid oxidizers. Acetate concentrations at 50% and 60% FOG were 353 ± 166 and 711 ± 227 mg L^{-1}, respectively (Table 4). Propionate concentrations were 650 ± 13 mg L^{-1} and 600 ± 60 mg L^{-1} for 50% and 60% FOG, respectively. Despite high VFAs, pH remained above 6.9 due to adequate carbonate buffering. Direct inhibition by VFAs was unlikely as other studies observed inhibition at significantly higher concentrations (Franke-Whittle et al., 2014). Therefore, VFA degrading populations were likely inhibited by LCFA or other components of FOG.

Using analysis of molecular variance (AMOVA), a significant variation ($p = 0.027$) in microbial community profiles was observed between substrate mixtures with high and low methane production. A non-metric multidimensional scaling (NMDS) plot of microbial community structure for 50% and 60% FOG clustered together (Fig. S17). Given that all substrate mixtures for Run 5 were seeded from Run 4 30% FOG+FW, similar microbial activities were observed at the beginning of Run 5 (Fig. 6). End of run samples from duplicate vessels submitted for RNA-based sequencing in Run 5 showed reproducibility of relative activity profiles, except at 40% FOG which also had inconsistent biogas production. Genus-level classification showed that unclassified *Clostridiales,* unclassified

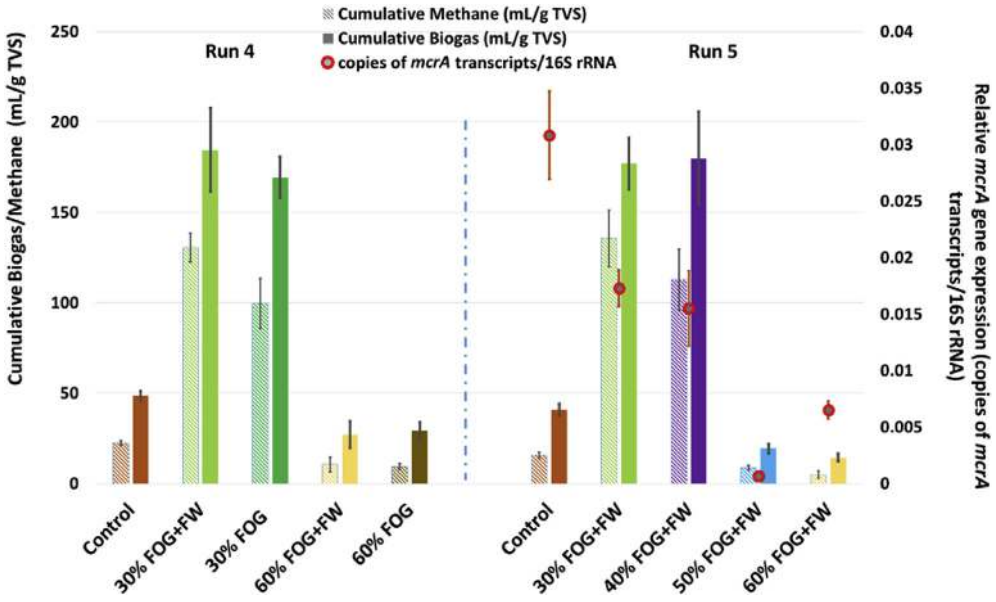

Fig. 5. Cumulative biogas (solid fill) and methane (pattern fill) with increasing FOG addition normalized to initial TVS loading. One of the triplicates vessels for 40% FOG showed an outlier in biogas production compared to the other replicates and was excluded from the mean analysis in this figure. Error bars for cumulative biogas/methane production indicate the combined standard deviation for gas production and initial organic loading in g TVS for triplicate vessels for each substrate mixture. The error bars for relative *mcrA* gene expression represent the standard deviation of the ratio of triplicate RT-qPCR reactions.

Thermotogales, Anaerobaculum, and *Syntrophomonas* were the most active OTUs at the lowest FOG loading. *Coprothermobacter* was also highly active at 30% and 40% FOG with high methane production, but relatively inactive at 50% and 60% FOG. *Coprothermobacter*, proteolytic anaerobic fermenters that have an optimum growth rate at 55 °C (Etchebehere et al., 1998), were positively correlated ($R = 0.890$, $p = 0.003$) with methane production (Table 5). *Thermotogales* followed a similar trend with high relative activity at 30% and 40% FOG and no activity at 50% and 60% FOG.

Several populations significantly increased in relative activity at high FOG OLR. For example, *Lactobacillus* and *Tepidimicrobium* had high relative activity at 50% and 60% FOG. Further, these populations were highly active at 40% FOG when biogas production was low (outlier in data set) but relatively inactive when biogas production was high (Fig. 6). Spearman rank analysis showed a negative correlation between methane production and relative activity of *Lactobacillus* ($R = -0.762$, $p = 0.028$). *Lactobacillus* have been shown to dominate in AD with FW (Shin et al., 2010), and also comprised 77.9% of the relative abundance and 86.0% of the relative activity in the raw FW samples sequenced in our study (Fig. S4). *Tepidimicrobium* spp., protein and amino acid degraders (Tang et al., 2011), may have been active at high FOG OLR because they had less competition from other populations inhibited by high LCFA. A previous study found a positive correlation between acetate and propionate concentrations and the presence of *Tepidimicrobium* (Regueiro et al., 2015), corroborating the observations here. LCFA accumulation likely occurred at 50% and 60% FOG because syntrophic-fatty acid oxidizers did not sufficiently increase activity, thereby resulting in inhibition of methanogens, similar to what was observed in a previous study (Ziels et al., 2016). The mechanism of LCFA toxicity on syntrophic-fatty acid oxidizers (e.g., biochemical inhibition or mass transfer limitations leading to decrease of cell permeability (Ma et al., 2015)), requires further investigation.

A significant positive correlation between the sum of the relative activity of syntrophic fatty-acid oxidizers and methane production was observed ($R = 0.909$ $p = 0.0017$; Table 5). Syntrophic fatty-acid oxidizers showed a remarkably high increase in relative activity at both 30% and 40% FOG (Fig. S18). These populations increased from 0.629% in the beginning of Run 5 to 19.5% and 21.3% in the two duplicate samples for 30% FOG at the end of Run 5 (Fig. 7B). *Syntrophomonas* and *Syntrophothermus* comprised the majority of this syntrophic relative activity. *Syntrophomonas* likely prevented the accumulation of LCFA at high FOG OLR. It has been previously proposed that prediction of FOG-loading capacity of a digester is possible by monitoring abundance of *Syntrophomonas* (Ziels et al., 2016) and that higher LCFA degradation rates were achieved with increased abundance of *Syntrophomonas* (Ziels et al., 2017). *Syntrophomonas* and *Syntrophothermus* showed significant positive correlation with methane production, both with R values of 0.792 (Table 5). Syntrophic fatty-acid oxidizers increased from

Table 4
TVS removal, free ammonia concentration, pH, VFA concentration, sulfate concentration, and sulfate reduction for end of Run 5. The detection limit for the IC analyses was 10 mg L^{-1}. The row marked 40% FOG* shows the results of the outlier sample in the 40% FOG condition.

	TVS reduction (%)	Free ammonia (mg L^{-1})	pH	Acetate (mg L^{-1})	Propionate (mg L^{-1})	Butyrate (mg L^{-1})	Formate (mg L^{-1})	Valerate (mg L^{-1})	Sulfate (mg L^{-1})	Sulfate reduction (%)
Control	13.4 ± 4.4	93.2 ± 24.9	7.70 ± 0.1	<10	160 ± 59	<10	<10	<10	28.8 ± 0.6	87.5 ± 0.279
30%FOG	51.8 ± 10.9	134 ± 50	7.70 ± 0.1	<10	<10	<10	<10	<10	40.0 ± 18.4	76.5 ± 9.91
40%FOG	53.2 ± 10.8	132 ± 2	7.50 ± 0.3	<10	<10	<10	<10	<10	75.7 ± 34.3	49.3 ± 27.2
50% FOG	57.7 ± 4.3	33.5 ± 7.0	7.10 ± 0.1	353 ± 166	650 ± 13	<10	121 ± 10.8	92.0 ± 4.10	14.5 ± 0.3	88.7 ± 0.2
60% FOG	60.8 ± 0.3	22.2 ± 12.3	6.90 ± 0.2	717 ± 227	600 ± 60	<10	139 ± 4.58	103 ± 1.60	14.3 ± 1.8	88.4 ± 1.7
40%FOG*	54.7	41.1 ± 6.3	7.13	325 ± 10.8	660 ± 2	<10	60.0 ± 65.7	80.1 ± 0.2	15.0 ± 0.03	90.0 ± 0.02

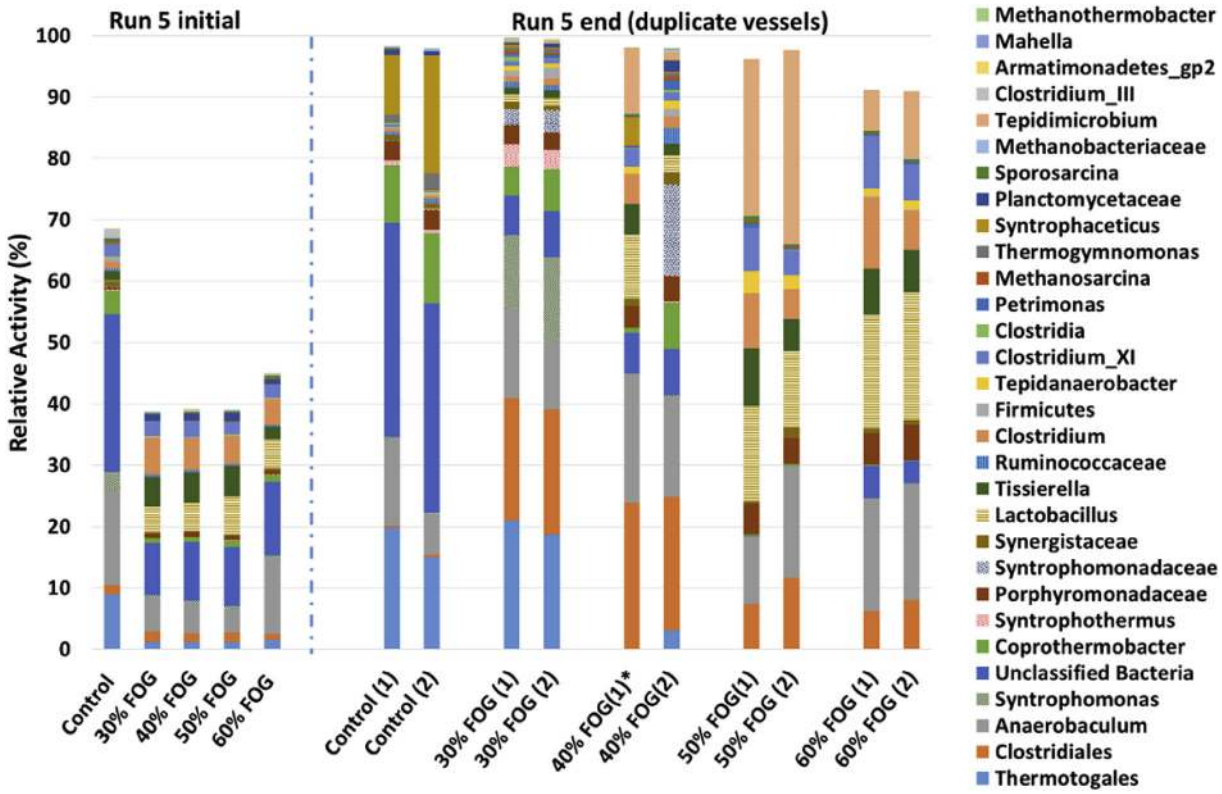

Fig. 6. Top 30 most active OTUs classified at the genus level for Run 5 (FOG inhibition study) at the beginning and end of run. Duplicate results are shown for the end of the run to represent methodological precision. 40% FOG(1)* shows results of a vessel with low biogas production. All data are expressed as a percentage normalized using total 16S rRNA sequences (*Bacteria* and *Archaea*).

0.467% at the beginning of Run 5 in biogas producing 40% FOG to 16.9% at the end of Run 5. The 40% FOG with low biogas production only showed an increase in relative activity of these populations to 5.83% at the end of Run 5, suggesting their importance. In sharp contrast, the relative activity of syntrophic fatty-acid oxidizers at 50% FOG was only 3.65% and 2.25% and even lower at 60% FOG, 1.3% and 1.47%. Further, neither *Syntrophomonas* nor *Syntrophothermus* were active at high FOG. The majority of syntrophic relative activity at 50% and 60% FOG was *Tepidanaerobacter,* a syntrophic acetate oxidizer. The significant increase in relative activity of key syntrophs at 30% and 40% FOG suggests that high FOG loading could be an important bioaugmentation strategy to boost these populations in AD. A study that used a CSTR to study the impact of FOG co-digestion reported up to 52% FOG (w/w) addition was not inhibitory throughout 198 days of operation (Ziels et al., 2016). Although Run 5 in our study was conducted for a shorter period (33 days), we reseeded biomass from the preceding run that had already acclimated to the high FOG addition. Therefore, reseeding likely compensated for the long lag phase needed at high concentrations of FOG. Notably, our study run time was similar to other batch reactors that investigated the impact of high FOG addition (Li et al. 2011, 2015; Martínez et al., 2011). Further, the use of RNA-based methods also added sensitivity relative to other studies that used DNA-based method (Ziels et al., 2016) to evaluate changes in the microbial community. Nevertheless, longer retention times may have eventually led to recovery in 50% FOG and 60% FOG vessels.

Table 5
Spearman rank correlation in Run 5 for methane production and microbial activity of prominent groups normalized to total 16S rRNA.

Group	R	*p*	Group	R	*p*
Planctomycetaceae	0.943	0.0004	*Sporosarcina*	−0.962	0.0001
Methanosarcina	0.909	0.002	*Tissierella*	−0.866	0.005
Coprothermobacter	0.890	0.003	*Clostridium*	−0.847	0.008
Syntrophomonadaceae	0.875	0.004	*Porphyromonadaceae*	−0.837	0.010
Thermogymnomonas	0.833	0.010	*Clostridium XI*	−0.812	0.014
Syntrophomonas	0.792	0.019	*Turicibacter*	−0.800	0.017
Syntrophothermus	0.792	0.019	*Ruminococcus*	−0.769	0.026
Clostridiales	0.788	0.020	*Lactobacillus*	−0.762	0.028
Petrimonas	0.752	0.032	*Tepidiphilus*	−0.762	0.028
Syntrophaceticus	0.749	0.032			
unclassified *Bacteria*	0.738	0.037			
Total Syntrophs	0.909	0.002			
Total Methanogens	0.738	0.037			

Relative activity of methanogens decreased significantly at high FOG OLR (Fig. 7A). However, *Methanoculleus* increased in relative activity suggesting more resilience or adaptation potential to high FOG. The only methanogen that showed significant positive correlation with methane production in the FOG inhibition study was *Methanosarcina* ($R = 0.909$, $p = 0.0017$) (Table 5). RT-qPCR targeting methanogen activity via *mcrA* gene expression indicated a steep decline in *mcrA* gene expression normalized to 16S rRNA at high FOG OLR, with total inhibition at 50% FOG (Fig. 5). A previous study demonstrated that high LCFA can impact the membrane integrity of methanogens (Sousa et al., 2013), and this could have been the mechanism of inhibition in our study. Trends in RT-qPCR results were similar to relative activity inferred from 16S rRNA sequencing and thus confirmed that 16S rRNA sequencing is a useful tool in profiling active methanogens.

The majority of previous studies evaluating FOG co-digestion have been at mesophilic temperatures (Long et al., 2012; Silvestre et al., 2011; Ziels et al., 2016), although thermophilic temperature

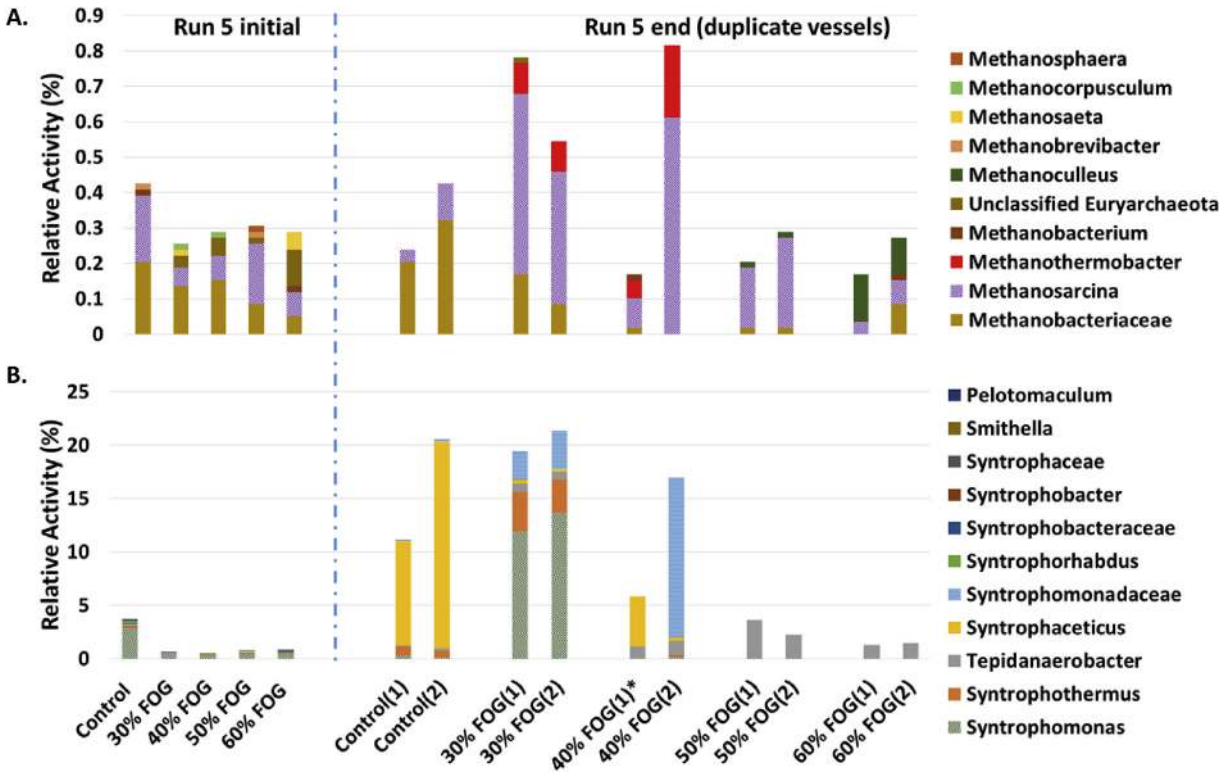

Fig. 7. **(A)** Relative activity of methanogens identified at the genus level based on 16S rRNA sequencing and **(B)** relative activity of syntrophic fatty-acid oxidizers identified at the genus level based on 16S rRNA sequencing. Results are expressed as percentages normalized to the total 16S rRNA sequences (*Bacteria* and *Archaea*). Duplicate results are shown for the end of the run to represent methodological precision. 40% FOG(1)* shows results of a vessel with low biogas production. Truncated y-axes (0–0.9% and 0–25% on figure A and B, respectively) are shown to accentuate differences in abundance.

has been reported to increase LCFA degradation, increase reaction rates, and promote faster liquid-solid separation (Yenigün and Demirel, 2013). The benefits of operating at thermophilic temperature compared to the increased energy demand for heating should be taken into consideration in full-scale applications (Long et al., 2012). The OLR of FOG addition without incurring inhibition has been a subject of various studies, with differing reports (Alqaralleh et al., 2016; Cirne et al., 2007; Rasit et al., 2015). For example, a study that conducted thermophilic and two stage hyperthermophilic reactors with co-digestion of TWAS and FOG reported inhibition at 80% FOG addition (TVS) (Alqaralleh et al., 2016). Some studies have suggested the addition of lipase-enzyme (Donoso-Bravo and Fdz-Polanco, 2013) and two-stage reactors (Li et al., 2015) to mitigate inhibition. Mitigation strategies should be further evaluated by including microbial community analyses to characterize the impact on active microbial populations, particularly on syntrophic bacteria that were highly impacted by high FOG addition in this study.

4. Conclusions

The impact of co-digestion of FW and FOG on performance and microbial community dynamics during bench-scale respirometry was evaluated using high-throughput DNA and RNA-based sequencing and RT-qPCR. The following conclusions were made based on observations during the study:

- Co-digestion of FOG and FW simultaneously increased performance by enhancing TVS removal and methane production; however, FOG addition was more impactful in increasing performance.
- FOG addition increased lag-phase significantly, which was reduced in later runs due to microbial community adaptation.
- Syntrophic fatty-acid oxidizers, such as *Syntrophomonas*, were enriched during co-digestion and were highly linked with increases in methane production, particularly at high FOG addition.
- 30% VSL FOG addition was optimal, where methane production was >50% that of PS+TWAS likely due to a 34 fold increase in relative activity of syntrophic fatty-acid oxidizers. However, FOG addition resulted in unstable performance and extreme inhibition at 50–60% VSL.
- Overall, AD performance in this study was better linked with syntrophic fatty-acid oxidizers than methanogens, suggesting the importance of evaluating these populations in full-scale reactors that perform co-digestion with FOG.

Acknowledgements

The authors wish to thank Judy Opp for help with Illumina sequencing. We would like to thank LA Sanitation and Divert, Inc. for their participation in the study. YMA was supported by a Provost Fellowship from the University of Southern California.

Appendix A. Supplementary data

Supplementary data related to this article can be found at http://dx.doi.org/10.1016/j.watres.2017.06.065.

References

Alqaralleh, R.M., Kennedy, K., Delatolla, R., Sartaj, M., 2016. Thermophilic and hyperthermophilic co-digestion of waste activated sludge and fat, oil and grease: evaluating and modeling methane production. J. Environ. Manag. 183, 551–561.

Amha, Y., Gregori, M., Johnson, B., Palacios, R.N., Smith, A.L., 2015a. Bench-and full-scale anaerobic co-digestion of fats oil and grease, food waste, and vegetable cooking oil for enhanced biogas production. Proc. Water Environ. Fed. 2015 (15), 5304–5311.

Amha, Y.M., Kumaraswamy, R., Ahmad, F., 2015b. A probabilistic QMRA of Salmonella in direct agricultural reuse of treated municipal wastewater. Water Sci. Technol. 71 (8), 1203–1211.

Becker, A.M., Yu, K., Stadler, L.B., Smith, A.L., 2017. Co-management of domestic wastewater and food waste: a life cycle comparison of alternative food waste diversion strategies. Bioresour. Technol. 223, 131–140.

Blazewicz, S.J., Barnard, R.L., Daly, R.A., Firestone, M.K., 2013. Evaluating rRNA as an indicator of microbial activity in environmental communities: limitations and uses. ISME J. 7 (11), 2061–2068.

Cirne, D., Paloumet, X., Björnsson, L., Alves, M., Mattiasson, B., 2007. Anaerobic digestion of lipid-rich waste—effects of lipid concentration. Renew. Energy 32 (6), 965–975.

Conklin, A., Stensel, H.D., Ferguson, J., 2006. Growth kinetics and competition between Methanosarcina and Methanosaeta in mesophilic anaerobic digestion. Water Environ. Res. 78 (5), 486–496.

Dai, X., Duan, N., Dong, B., Dai, L., 2013. High-solids anaerobic co-digestion of sewage sludge and food waste in comparison with mono digestions: stability and performance. Waste Manag. 33 (2), 308–316.

Davidsson, Å., Lövstedt, C., la Cour Jansen, J., Gruvberger, C., Aspegren, H., 2008. Co-digestion of grease trap sludge and sewage sludge. Waste Manag. 28 (6), 986–992.

De Vrieze, J., Regueiro, L., Props, R., Vilchez-Vargas, R., Jáuregui, R., Pieper, D.H., Lema, J.M., Carballa, M., 2016. Presence does not imply activity: DNA and RNA patterns differ in response to salt perturbation in anaerobic digestion. Biotechnol. Biofuels 9 (1), 244.

Donoso-Bravo, A., Fdz-Polanco, M., 2013. Anaerobic co-digestion of sewage sludge and grease trap: assessment of enzyme addition. Process Biochem. 48 (5), 936–940.

Duan, N., Dong, B., Wu, B., Dai, X., 2012. High-solid anaerobic digestion of sewage sludge under mesophilic conditions: feasibility study. Bioresour. Technol. 104, 150–156.

Etchebehere, C., Pavan, M., Zorzopulos, J., Soubes, M., Muxi, L., 1998. Coprothermobacter platensis sp. nov., a new anaerobic proteolytic thermophilic bacterium isolated from an anaerobic mesophilic sludge. Int. J. Syst. Evol. Microbiol. 48 (4), 1297–1304.

Franke-Whittle, I.H., Walter, A., Ebner, C., Insam, H., 2014. Investigation into the effect of high concentrations of volatile fatty acids in anaerobic digestion on methanogenic communities. Waste Manag. 34, 2080–2089.

Girault, R., Bridoux, G., Nauleau, F., Poullain, C., Buffet, J., Peu, P., Sadowski, A.G., Béline, F., 2012. Anaerobic co-digestion of waste activated sludge and greasy sludge from flotation process: batch versus CSTR experiments to investigate optimal design. Bioresour. Technol. 105, 1–8.

Hansen, K.H., Angelidaki, I., Ahring, B.K., 1998. Anaerobic digestion of swine manure: inhibition by ammonia. Water Res. 32 (1), 5–12.

Hao, L.-P., Lü, F., He, P.-J., Li, L., Shao, L.-M., 2010. Predominant contribution of syntrophic acetate oxidation to thermophilic methane formation at high acetate concentrations. Environ. Sci. Technol. 45 (2), 508–513.

Hatamoto, M., Imachi, H., Yashiro, Y., Ohashi, A., Harada, H., 2007. Diversity of anaerobic microorganisms involved in long-chain fatty acid degradation in methanogenic sludges as revealed by RNA-based stable isotope probing. Appl. Environ. Microbiol. 73 (13), 4119–4127.

Hattori, S., 2008. Syntrophic acetate-oxidizing microbes in methanogenic environments. Microbes Environ. 23 (2), 118–127.

Kabouris, J.C., Tezel, U., Pavlostathis, S.G., Engelmann, M., Dulaney, J.A., Todd, A.C., Gillette, R.A., 2009. Mesophilic and thermophilic anaerobic digestion of municipal sludge and fat, oil, and grease. Water Environ. Res. 81 (5), 476–485.

Karakashev, D., Batstone, D.J., Angelidaki, I., 2005. Influence of environmental conditions on methanogenic compositions in anaerobic biogas reactors. Appl. Environ. Microbiol. 71 (1), 331–338.

Klappenbach, J.A., Dunbar, J.M., Schmidt, T.M., 2000. rRNA operon copy number reflects ecological strategies of bacteria. Appl. Environ. Microbiol. 66 (4), 1328–1333.

Koch, K., Helmreich, B., Drewes, J.E., 2015. Co-digestion of food waste in municipal wastewater treatment plants: effect of different mixtures on methane yield and hydrolysis rate constant. Appl. Energy 137, 250–255.

Koch, K., Plabst, M., Schmidt, A., Helmreich, B., Drewes, J.E., 2016. Co-digestion of food waste in a municipal wastewater treatment plant: comparison of batch tests and full-scale experiences. Waste Manag. 47 (Part A), 28–33.

Kong, Dung, et al., 2012. Evaluating greenhouse gas impacts of organic waste management options using life cycle assessment. Waste Manag. Res. 30 (8), 800–812.

Kumaraswamy, R., Amha, Y.M., Anwar, M.Z., Henschel, A., Rodríguez, J., Ahmad, F., 2014. Molecular analysis for screening human bacterial pathogens in municipal wastewater treatment and reuse. Environ. Sci. Technol. 48 (19), 11610–11619.

Lee, S.-H., Park, J.-H., Kim, S.-H., Yu, B.J., Yoon, J.-J., Park, H.-D., 2015. Evidence of syntrophic acetate oxidation by Spirochaetes during anaerobic methane production. Bioresour. Technol. 190, 543–549.

Leibrock, A., 2017. Are Food Waste Bans Working?.

Leinonen, Rasko, Sugawara, Hideaki, Shumway, Martin, on behalf of the International Nucleotide Sequence Database Collaboration, 2011. The sequence read archive. Nucleic Acids Res. 39 (suppl. 1), D19–D21. http://dx.doi.org/10.1093/nar/gkq1019.

Li, C., Champagne, P., Anderson, B., 2015. Enhanced biogas production from anaerobic co-digestion of municipal wastewater treatment sludge and fat, oil and grease (FOG) by a modified two-stage thermophilic digester system with selected thermo-chemical pre-treatment. Renew. Energy 83, 474–482.

Li, C., Champagne, P., Anderson, B.C., 2011. Evaluating and modeling biogas production from municipal fat, oil, and grease and synthetic kitchen waste in anaerobic co-digestions. Bioresour. Technol. 102 (20), 9471–9480.

Li, L., He, Q., Ma, Y., Wang, X., Peng, X., 2016. A mesophilic anaerobic digester for treating food waste: process stability and microbial community analysis using pyrosequencing. Microb. Cell Factories 15 (1), 65.

Long, J.H., Aziz, T.N., Francis, L., Ducoste, J.J., 2012. Anaerobic co-digestion of fat, oil, and grease (FOG): a review of gas production and process limitations. Process Saf. Environ. Prot. 90 (3), 231–245.

Ma, J., Zhao, Q.-B., Laurens, L.L.M., Jarvis, E.E., Nagle, N.J., Chen, S., Frear, C.S., 2015. Mechanism, kinetics and microbiology of inhibition caused by long-chain fatty acids in anaerobic digestion of algal biomass. Biotechnol. Biofuels 8 (1), 141.

Martín-González, L., Castro, R., Pereira, M.A., Alves, M.M., Font, X., Vicent, T., 2011. Thermophilic co-digestion of organic fraction of municipal solid wastes with FOG wastes from a sewage treatment plant: reactor performance and microbial community monitoring. Bioresour. Technol. 102 (7), 4734–4741.

Martínez, E.J., Redondas, V., Fierro, J., Gómez, X., Morán, A., 2011. Anaerobic digestion of high lipid content wastes: FOG co-digestion and milk processing fat digestion. J. Residuals Sci. Technol. 8 (2).

Matteson, G.C., Jenkins, B., 2007. Food and processing residues in California: Resource assessment and potential for power generation. Bioresour. Technol. 98 (16), 3098–3105.

Mladenovska, Z., Ahring, B.K., 1997. Mixotrophic growth of two thermophilic Methanosarcina strains, Methanosarcina thermophila TM-1 and Methanosarcina sp. SO-2P, on methanol and hydrogen/carbon dioxide. Appl. Microbiol. Biotechnol. 48 (3), 385–388.

Morris, R., Schauer-Gimenez, A., Bhattad, U., Kearney, C., Struble, C.A., Zitomer, D., Maki, J.S., 2014. Methyl coenzyme M reductase (mcrA) gene abundance correlates with activity measurements of methanogenic H2/CO2-enriched anaerobic biomass. Microb. Biotechnol. 7 (1), 77–84.

Mosbæk, F., Kjeldal, H., Mulat, D.G., Albertsen, M., Ward, A.J., Feilberg, A., Nielsen, J.L., 2016. Identification of syntrophic acetate-oxidizing bacteria in anaerobic digesters by combined protein-based stable isotope probing and metagenomics. ISME J. http://dx.doi.org/10.1038/ismej.2016.39.

Narihiro, T., Nobu, M.K., Kim, N.K., Kamagata, Y., Liu, W.T., 2015. The nexus of syntrophy-associated microbiota in anaerobic digestion revealed by long-term enrichment and community survey. Environ. Microbiol. 17 (5), 1707–1720.

Noutsopoulos, C., Mamais, D., Antoniou, K., Avramides, C., Oikonomopoulos, P., Fountoulakis, I., 2013. Anaerobic co-digestion of grease sludge and sewage sludge: the effect of organic loading and grease sludge content. Bioresour. Technol. 131, 452–459.

Palatsi, J., Illa, J., Prenafeta-Boldú, F., Laureni, M., Fernandez, B., Angelidaki, I., Flotats, X., 2010. Long-chain fatty acids inhibition and adaptation process in anaerobic thermophilic digestion: batch tests, microbial community structure and mathematical modelling. Bioresour. Technol. 101 (7), 2243–2251.

Platt, B., Goldstein, N., Coker, C., Brown, S., 2014. State of Composting in the US. Institute for Local Self-Reliance.

Props, R., Kerckhof, F.-M., Rubbens, P., De Vrieze, J., Sanabria, E.H., Waegeman, W., Monsieurs, P., Hammes, F., Boon, N., 2016. Absolute quantification of microbial taxon abundances. ISME J 11, 584–587. http://dx.doi.org/10.1038/ismej.2016.117.

Rasit, N., Idris, A., Harun, R., Ghani, W.A.W.A.K., 2015. Effects of lipid inhibition on biogas production of anaerobic digestion from oily effluents and sludges: an overview. Renew. Sustain. Energy Rev. 45, 351–358.

Regueiro, L., Lema, J.M., Carballa, M., 2015. Key microbial communities steering the functioning of anaerobic digesters during hydraulic and organic overloading shocks. Bioresour. Technol. 197, 208–216.

Salter, S.J., Cox, M.J., Turek, E.M., Calus, S.T., Cookson, W.O., Moffatt, M.F., Turner, P., Parkhill, J., Loman, N.J., Walker, A.W., 2014. Reagent and laboratory contamination can critically impact sequence-based microbiome analyses. BMC Biol. 12 (1), 1.

Schloss, P.D., Westcott, S.L., Ryabin, T., Hall, J.R., Hartmann, M., Hollister, E.B., Lesniewski, R.A., Oakley, B.B., Parks, D.H., Robinson, C.J., 2009. Introducing mothur: open-source, platform-independent, community-supported software for describing and comparing microbial communities. Appl. Environ. Microbiol. 75 (23), 7537–7541.

Schnürer, A., Schink, B., Svensson, B.H., 1996. Clostridium ultunense sp. nov., a mesophilic bacterium oxidizing acetate in syntrophic association with a hydrogenotrophic methanogenic bacterium. Int. J. Syst. Evol. Microbiol. 46 (4), 1145–1152.

Sekiguchi, Y., Kamagata, Y., Nakamura, K., Ohashi, A., Harada, H., 2000. Syntrophothermus lipocalidus gen. nov., sp. nov., a novel thermophilic, syntrophic, fatty-acid-oxidizing anaerobe which utilizes isobutyrate. Int. J. Syst. Evol. Microbiol. 50 (2), 771–779.

Shin, S.G., Han, G., Lim, J., Lee, C., Hwang, S., 2010. A comprehensive microbial insight into two-stage anaerobic digestion of food waste-recycling wastewater. Water Res. 44 (17), 4838–4849.

Silva, S.A., Cavaleiro, A.J., Pereira, M.A., Stams, A.J.M., Alves, M.M., Sousa, D.Z., 2014. Long-term acclimation of anaerobic sludges for high-rate methanogenesis from LCFA. Biomass Bioenergy 67, 297–303.

Silvestre, G., Rodríguez-Abalde, A., Fernández, B., Flotats, X., Bonmatí, A., 2011. Biomass adaptation over anaerobic co-digestion of sewage sludge and trapped grease waste. Bioresour. Technol. 102 (13), 6830–6836.
Smith, A.L., Skerlos, S.J., Raskin, L., 2015. Membrane biofilm development improves COD removal in anaerobic membrane bioreactor wastewater treatment. Microb. Biotechnol. 8 (5), 883–894.
Sousa, D.Z., Salvador, A.F., Ramos, J., Guedes, A.P., Barbosa, S., Stams, A.J.M., Alves, M.M., Pereira, M.A., 2013. Activity and viability of methanogens in anaerobic digestion of unsaturated and saturated long-chain fatty acids. Appl. Environ. Microbiol. 79 (14), 4239–4245.
Sousa, D.Z., Smidt, H., Alves, M.M., Stams, A.J.M., 2009. Ecophysiology of syntrophic communities that degrade saturated and unsaturated long-chain fatty acids. FEMS Microbiol. Ecol. 68 (3), 257–272.
Sundberg, C., Al-Soud, W.A., Larsson, M., Alm, E., Yekta, S.S., Svensson, B.H., Sørensen, S.J., Karlsson, A., 2013. 454 pyrosequencing analyses of bacterial and archaeal richness in 21 full-scale biogas digesters. FEMS Microbiol. Ecol. 85 (3), 612–626.
Tang, Y.-Q., Ji, P., Hayashi, J., Koike, Y., Wu, X.-L., Kida, K., 2011. Characteristic microbial community of a dry thermophilic methanogenic digester: its long-term stability and change with feeding. Appl. Microbiol. Biotechnol. 91 (5), 1447–1461.
Wang, L., Aziz, T.N., Francis, L., 2013. Determining the limits of anaerobic co-digestion of thickened waste activated sludge with grease interceptor waste. Water Res. 47 (11), 3835–3844.
Welander, P.V., Metcalf, W.W., 2005. Loss of the mtr operon in Methanosarcina blocks growth on methanol, but not methanogenesis, and reveals an unknown methanogenic pathway. Proc. Natl. Acad. Sci. U. S. A. 102 (30), 10664–10669.
Werner, J.J., Garcia, M.L., Perkins, S.D., Yarasheski, K.E., Smith, S.R., Muegge, B.D., Stadermann, F.J., DeRito, C.M., Floss, C., Madsen, E.L., 2014. Microbial community dynamics and stability during an ammonia-induced shift to syntrophic acetate oxidation. Appl. Environ. Microbiol. 80 (11), 3375–3383.
Westerholm, M., Dolfing, J., Sherry, A., Gray, N.D., Head, I.M., Schnürer, A., 2011. Quantification of syntrophic acetate-oxidizing microbial communities in biogas processes. Environ. Microbiol. Rep. 3 (4), 500–505.
Wu, L.-J., Kobayashi, T., Kuramochi, H., Li, Y.-Y., Xu, K.-Q., 2016. Improved biogas production from food waste by co-digestion with de-oiled grease trap waste. Bioresour. Technol. 201, 237–244.
Xu, R., Yang, Z., Chen, T., Zhao, L., Huang, J., Xu, H., Song, P., Li, M., 2015. Anaerobic co-digestion of municipal wastewater sludge with food waste with different fat, oil, and grease contents: study of reactor performance and extracellular polymeric substances. RSC Adv. 5 (125), 103547–103556.
Yang, Z.-H., Xu, R., Zheng, Y., Chen, T., Zhao, L.-J., Li, M., 2016. Characterization of extracellular polymeric substances and microbial diversity in anaerobic co-digestion reactor treated sewage sludge with fat, oil, grease. Bioresour. Technol. 212, 164–173.
Yenigün, O., Demirel, B., 2013. Ammonia inhibition in anaerobic digestion: a review. Process Biochem. 48 (5), 901–911.
Zhu, X., De Francisci, D., Treu, L., Kougias, P., Campanaro, S., Angelidaki, I., 2015. Metagenomic analysis on thermophilic biogas reactors fed with high load of Long Chain Fatty Acids (LCFA). In: Proceedings of the 14th World Congress on Anaerobic Digestion.
Ziels, R.M., Beck, D.A.C., Martí, M., Gough, H.L., Stensel, H.D., Svensson, B.H., 2015. Monitoring the dynamics of syntrophic β-oxidizing bacteria during anaerobic degradation of oleic acid by quantitative PCR. FEMS Microbiol. Ecol. 91 (4), fiv028.
Ziels, R.M., Beck, D.A.C., Stensel, H.D., 2017. Long-chain fatty acid feeding frequency in anaerobic codigestion impacts syntrophic community structure and biokinetics. Water Res. 117, 218–229.
Ziels, R.M., Karlsson, A., Beck, D.A.C., Ejlertsson, J., Yekta, S.S., Bjorn, A., Stensel, H.D., Svensson, B.H., 2016. Microbial community adaptation influences long-chain fatty acid conversion during anaerobic codigestion of fats, oils, and grease with municipal sludge. Water Res. 103, 372–382.